Title Page

Non-redundant contribution of the plastidial FAD8 ω-3 desaturase to glycerolipid unsaturation at different temperatures in *Arabidopsis*

Ángela Román[1,2], María L. Hernández[2], Ángel Soria-García[1], Sara López-Gomollón[1], Beatriz Lagunas[1], Rafael Picorel[1], José Manuel Martínez-Rivas[2], and Miguel Alfonso[1,*]

[1] Estación Experimental de Aula Dei (EEAD-CSIC). Avda. Montañana 1005, 50059 Zaragoza (Spain).

[2] Instituto de la Grasa (IG-CSIC). Campus Universidad Pablo de Olavide, Building 46, Ctra. Utrera km.1, 41013 Sevilla (Spain).

[*] To whom correspondence should be addressed: Miguel Alfonso; EEAD-CSIC, Avda. Montañana 1005, 50059 Zaragoza. Phone: 34-976-716059; FAX: 34-976-716145; E-mail: alfonso@eead.csic.es

Running Title: non-redundant role of FAD8 on lipid unsaturation

Short summary: The plastidial ω-3 desaturase FAD8 showed activity at growth temperature, with higher selectivity for 18:2 acyl-lipid substrates and a higher preference for PG. These results suggest that the activity of FAD8 and FAD7 plastidial desaturases is controlled in a non-redundant manner.

ABSTRACT The plastidial ω-3 desaturase FAD7 is the major contributor to trienoic fatty acid biosynthesis in leaves. However, the precise contribution of the other plastidial ω-3 desaturase, FAD8, is poorly understood. Fatty acid and lipid analysis in several ω-3 desaturase mutants, including two insertion *AtFAD7* and *AtFAD8* lines, showed that FAD8 partially compensated the disruption of the *AtFAD7* gene at 22 ºC, indicating that FAD8 was active at that growth temperature. These results contrasted with previous observations that circumscribed FAD8 activity to low temperatures. Our data revealed that FAD8 had a higher selectivity for 18:2 acyl-lipid substrates and a higher preference for lipids other than galactolipids, concretely PG, at any of the temperatures studied. Differences in the mechanism controlling *AtFAD7* and *AtFAD8* gene expression at different temperatures were also detected. Confocal microscopy and biochemical analysis of FAD8-YFP over-expressing lines confirmed the chloroplast envelope localization of FAD8. Co-localization experiments suggested that FAD8 and FAD7 might be located in close vicinity in the envelope membrane. FAD8-YFP over-expressing lines showed a specific increase of 18:3 at 22 ºC, confirming the results obtained with the mutants. These results all-together indicated that the function of both plastidial ω-3 desaturases is coordinated in a non-redundant manner.

Keywords: *Arabidopsis thaliana*, glycerolipid, fatty acid, desaturase, FAD7, FAD8, plastid.

INTRODUCTION

Fatty acids are the major constituents of membrane lipids. In plants, trienoic (TA) and dienoic (DA) fatty acids represent up to 70% of total fatty acids from leaf polar lipids. Most of these fatty acids are esterified to galactolipids, which are the main lipid species found in leaf chloroplasts (Browse *et al.,* 1986; Browse and Somerville, 1991). Desaturase activity responsible for polyunsaturated fatty acid biosynthesis was initially detected in microsomal and plastidial preparations of various plant tissues (Schmidt and Heinz, 1990; Ohlrogge and Browse, 1995). However, the hydrophobic nature of these desaturases complicated their analysis by biochemical methods. The molecular characterization of a collection of mutants from Arabidopsis, defective in membrane lipid unsaturation, allowed the identification of genes encoding fatty acid desaturases and provided specific knowledge about their number, substrate specificity and predicted location (reviewed in Wallis and Browse, 2002). Thus, TAs are synthesized from DAs by the activity of ω-3 fatty acid desaturases, which are a family of integral membrane enzymes located in two different cell compartments; FAD3 is localized in the endoplasmic reticulum (ER), (Dyer and Mullen, 2001) while FAD7 and FAD8 are plastid specific (Browse *et al.*, 1986; Wallis and Browse, 2002; Andreu *et al.,* 2007). These ω-3 fatty acid desaturases are encoded by nuclear genes. In Arabidopsis, a single gene encodes for each of these enzymes (Yadav *et al.*, 1993; Gibson *et al.*, 1994). In other plant species, like soybean (*Glycine max*) or flax (*Linum usitatissimum*), several isoforms of FAD3 have been detected (Bilyeu *et al.*, 2003; Vrinten *et al.*, 2005). More recently, two different genes encoding isoforms of FAD7 (*GmFAD7-1 and GmFAD7-2)* and FAD8 (*GmFAD8-1 and GmFAD8-2)* enzymes have been reported in soybean (Andreu *et al.*, 2010; Román *et al.,* 2012), being the only case in which isoforms have been identified for both plastidial ω-3 desaturases. Interestingly, the expression profiles of these genes showed differences in response to plant development, temperature or wounding, suggesting a high degree of specialization between isoforms in soybean (Andreu *et al.*, 2010; Román *et al.,* 2012; Lagunas *et al.,* 2013).

Since its discovery in Arabidopsis (Gibson *et al.*, 1994) the *FAD8* gene has been identified in many plant species (Berberich *et al.*, 1998; Wang *et al.*, 2006; Martz *et al.*, 2006; Tang *et al.*, 2007; Torres-Franklin *et al.*, 2009; Román *et al.*, 2012) and, in all cases, the homology with FAD7 was very high. Recently, it was reported that *CrFAD7*

is the only ω-3 fatty acid desaturase active in the chloroplast in the green alga *Chlamydomonas reinhardtii*, (Nguyen *et al.*, 2013). The question arises why plants retained during evolution two highly homologous ω-3 fatty acid desaturases in the same cell compartment and which is the precise role of FAD8. In Arabidopsis, a *fad8* mutant showed no significant changes in its fatty acid profile at control (22 ºC) temperature (McConn *et al.*, 1994). Furthermore, the phenotypic analysis of a *fad7* mutant from Arabidopsis showed that the reduction of TA levels caused by the *fad7* mutation was less pronounced at low temperatures (15 ºC), (McConn *et al.*, 1994). These results lead to the conclusion that FAD8 was largely irrelevant to lipid metabolism at control temperatures (22 ºC) in Arabidopsis, and that its activity was circumscribed to low temperatures (McConn *et al.*, 1994). However, it is not clear at present to which extent FAD8 activity substitutes totally or partially that from FAD7 at low temperatures. Although changes in *FAD8* transcripts in response to low temperatures (ranging from 5 ºC to 15 ºC) have been reported in many plant species like maize (Berberich *et al.*, 1998), rice (Wang *et al.*, 2006), birch (Martz *et al.*, 2006) or *Descurainia sophia* (Tang *et al.*, 2007) only in a few cases the expression profiles of the *FAD8* genes and the TA content were monitored simultaneously. When this was done, changes in *FAD8* expression were accompanied by small changes in TA content (McConn *et al.*, 1994; Martz *et al.*, 2006), indicating that this additional cold-induced FAD8 activity was not very high. Similarly, there is no direct evidence supporting that the role of FAD8 is exclusively restricted to low temperatures. In fact, the *FAD8* transcript has been detected in most plants analyzed at control growth temperatures (i.e., 22 - 25 ºC), (Gibson *et al.*, 1994; Matsuda *et al.*, 2005; Wang *et al.*, 2006; Martz *et al.*, 2006; Tang *et al.*, 2007; Torres-Franklin *et al.*, 2009; Román *et al.*, 2012). In the absence of biochemical data, that might determine the amount and activity of these ω-3 desaturases, we cannot preclude that this *FAD8* mRNA is translated into an active enzyme at control growth temperatures. Therefore, we still far from understand how FAD7 and FAD8 desaturases are coordinated to maintain an appropriate unsaturation level of membrane lipids at different temperatures.

In this work, we characterized the different contribution of FAD8 and FAD7 to TA biosynthesis in Arabidopsis at control (22 ºC), low (8 ºC) and high (30 ºC) temperatures. To that end, several mutant lines including two Salk insertion lines mutated at the *AtFAD7* and *AtFAD8* genes (*fad7i* and *fad8i*) together with a double *fad7*

fad8 mutant and a triple *fad3 fad7 fad8* mutant were functionally characterized. Our data suggest that the function of the FAD8 protein in Arabidopsis might not be redundant with respect to that of FAD7, not only regarding differences in the effects of temperature on gene expression, but also with respect to preference of acyl-group chain length and lipid head groups. In parallel, stable Arabidopsis transgenic lines over-expressing the FAD8 protein fused to YFP were characterized to investigate FAD8 function at the protein level. Confocal microscopy analysis of FAD8-YFP transgenic lines and biochemical fractionation of sub-chloroplast membranes confirmed the envelope localization of the FAD8 desaturase. Furthermore, co-localization analysis suggested that both plastidial ω-3 desaturases might be located in close vicinity in the envelope membrane. The fatty acid analysis of these FAD8 over-expressing plant lines showed specific ω-3 desaturase activity that confirmed the non-redundant role of FAD8 in the glycerolipid unsaturation pathway.

RESULTS

Molecular characterization of Arabidopsis *fad7* and *fad8* insertion lines

Search of single *fad7* and *fad8* EMS mutants at the NASC repository resulted in a single *fad7* mutant (N8042) but no single *fad8* locus accession. On the contrary, several T-DNA insertion lines mutated in the plastidial ω-3 desaturases were recovered from the NASC repository. Only two of them showed insertions exclusively in the *AtFAD7* (*At3g11370*) or *AtFAD8* (*At5g05560*) genes and were further characterized. These lines were SALK_147096C, designated as *fad7i,* and SALK_093590, designated as *fad8i*. Genomic analysis of *fad7i* plants revealed two insertions of an inverted tandem T-DNA in the *AtFAD7* gene; one located at 6 bp downstream of the exon 7 and the other one located within the intron 6, at 8 bp downstream of the end of exon 6 (Figure 1A). The genomic analysis of *fad8i* plants showed an insertion of an inverted tandem T-DNA 133 bp downstream of the start codon, within exon 1 of the *AtFAD8* gene (Figure 1A). RT-PCR characterization of two-week old *fad7i* and *fad8i* plants indicated the absence of the *AtFAD7* and *AtFAD8* transcripts in the corresponding mutants (Figure 1B). Homozygous *fad7i* and *fad8i* mutant lines were segregated and further analyzed. None of *fad7i* and *fad8i* plants showed any significant alterations in growth at control temperatures, developing normal rosette leaves. They germinated normally and grew in soil, producing seeds as the rest of the plant lines used in this study with the exception of the *fad3 fad7 fad8* mutant, which was sterile and did not produce seeds except if treated with jasmonic acid (McConn and Browse, 1996). The *fad7 fad8* and *fad3 fad7 fad8* mutants have been previously described (McConn *et al.*, 1994; McConn and Browse, 1996). They derived from single EMS mutants that were crossed to obtain both the double *fad7 fad8* and triple *fad3 fad7 fad8* mutants. We further characterized these mutants at the genetic level. The *fad8* mutation from the *fad7 fad8* double mutant had been previously characterized (Gibson *et al.*, 1994). Sequencing of the *AtFAD8* gene in either genomic or cDNA from the double *fad7 fad8* mutant confirmed these results, showing a point mutation of G (W residue) for A (STOP codon) substitution in residue 149 of the FAD8 protein. On the contrary, we were not able to find any sequencing data of the *fad7* mutation. Sequencing of the *AtFAD7* gene in either genomic or cDNA from the double *fad7 fad8* mutant showed a point mutation that introduced a substitution of G (W residue) for A (STOP codon) in residue 141 of the FAD7 protein. Sequencing analysis of the *AtFAD7* and *AtFAD8* genes in the triple mutant showed identical

substitutions to those found in the double *fad7 fad8* mutant. Finally, sequencing of the *AtFAD3* gene (*At2g29980*) in the *fad3 fad7 fad8* mutant resulted in a mutation of G for A. This introduced a substitution of C for Y in residue 103 of the mature protein. It is worth mentioning that this residue is part of the first His box essential for desaturase function.

Leaf lipid analysis of the Arabidopsis ω-3 desaturase mutant lines at growth temperature (22 ºC)

We analyzed the fatty acid composition of total leaf lipids from Col-0 and the different mutant lines grown at 22 ºC for four weeks (Figure 2A). TA average levels in Col-0 were 40.1% of linolenic acid (18:3) and 8.6% of hexadecatrienoic acid (16:3). A 16.7% of linoleic (18:2) and 1.8% of hexadecadienoic acid (16:2) were also detected (Figure 2A). These values were within the range previously observed for the Col-0 line (Gibson *et al.*, 1994; McConn *et al.*, 1994). Disruption of the *AtFAD7* gene in the *fad7i* mutant resulted in a reduction of TAs with an 18:3 content of 29.6% and an even more reduced content of 16:3 down to 2% (Figure 2A). These average percentages indicated that *fad7i* maintained 74% of 18:3 production with respect to Col-0 while only 23% of 16:3 synthesis was maintained in this mutant. On the contrary, the disruption of the *AtFAD8* gene in *fad8i* resulted in almost similar TA levels to those from Col-0 (Figure 2A). The *fad7 fad8* double mutant also showed a considerable reduction in TA, particularly in 16:3, which was undetectable (Figure 2A). Levels of 18:3 were also reduced to 12.3% in this mutant (Figure 2A), indicating that in the absence of plastidial ω-3 desaturase activity, FAD3 accounted for approximately 30% of the synthesized 18:3 with respect to that from Col-0. It is worth mentioning that this reduction in TAs was even greater than that previously reported in Gibson *et al.*, (1994) for their double *fad7 fad8* mutant. Finally, the *fad3 fad7 fad8* triple mutant showed no accumulation of TAs, consistent with the disruption of all ω-3 fatty acid desaturase genes (Figure 2A). The absence of TAs was accompanied by a strong increase of DAs, which reached average percentages of 68.5% of 18:2 and 10% of 16:2. Given the strong reduction (70%) in 18:3 content observed in the *fad7 fad8* double mutant, the data obtained in *fad7i* indicated that, after disruption of the *AtFAD7* gene, FAD8 enzymatic activity was able to maintain, at least partially (43.7%), the amount of 18:3 and to a much lesser extent (23.2%) that of 16:3 at 22 ºC (Figure 2A).

To investigate in more detail the effect of the disruption of the *AtFAD7* and *AtFAD8* genes on the lipid profiles, polar lipid classes were separated by bi-dimensional thin-layer chromatography (2D-TLC) and their fatty acid composition determined by gas chromatography (GC). Lipid composition in the Col-0 plants was similar to that reported previously (McConn *et al.,* 1994). No relevant modifications in the amount of lipids were observed in the different mutant lines at 22 ºC (see supplementary table S1). This result is consistent with previous observations in other fatty acid desaturase mutants (Miquel and Browse, 1992; Browse *et al.,* 1993; McConn *et al.,* 1994). The fatty acid composition of each lipid class in Col-0 and mutant lines is shown in the supplementary Table S1. Monogalactosyldiacylglycerol (MGDG) showed a high content of 18:3 and 16:3 in Col-0, with percentages of 59% and 28.2%, respectively (Figure 2B). The MGDG from the *fad7i* mutant showed a 48% and 82% reduction of 18:3 and 16:3, respectively, when compared to Col-0, whereas the disruption of the *AtFAD8* gene resulted in minor changes in the fatty acid composition of MGDG (Figure 2B). As observed in total lipids, very low amounts of 18:3 (7% from total) were detected in MGDG from the *fad7 fad8* double mutant while 16:3 was undetectable (Figure 2B). Similarly, neither 16:3 nor 18:3 were detected in the *fad3 fad7 fad8* triple mutant (Figure 2B). Comparison of the TA content in MGDG of the *fad7i*, *fad8i* and *fad7 fad8* mutants at 22 ºC indicated that in *fad7i*, FAD8 activity was capable to partially maintain the 18:3 content of MGDG, while its capacity to maintain 16:3 levels was very much reduced. A similar conclusion could be reached from the analysis of digalactosyldiacylglycerol (DGDG) or phosphatidylcholine (PC), having in mind that DGDG has highly reduced 16:3 levels even in Col-0 and PC has no 16:3 (Figure 2B). On the contrary, different results were obtained when phosphatidylglycerol (PG) was analyzed. As shown in Figure 2B, 18:3 levels in Col-0 PG were around 27.3%, while in the *fad7i* mutant, it reached 17.8%, which meant a 33% reduction when compared to Col-0 (Figure 2B). Interestingly, disruption of the *AtFAD8* gene resulted in even lower levels of 18:3 in PG of 13% from total fatty acids (i.e., a 56% reduction with respect to Col-0; Figure 2B). An even stronger reduction of 77% (from 27 to 6%) was observed in PG from the *fad7 fad8* double mutant (Figure 2B). This 18:3 PG found in the *fad7 fad8* double mutant probably originated from extraplastidial biosynthesis of PG in the ER (Frentzen, 2004). Finally, no 18:3 was detected in PG from the *fad3 fad7 fad8* triple mutant. These results suggested that at 22 ºC, disruption of the *AtFAD8* gene affected more the 18:3 content of the PG fraction than that of the *AtFAD7* gene.

Effect of temperature on leaf lipids of the Arabidopsis ω-3 desaturase mutants

The effect of low (8 ºC) and high (30 ºC) temperatures on leaf lipid fatty acid composition in Col-0 and the different mutant lines was also investigated. No significant modifications in the leaf 18:3 content from total lipids isolated from Col-0 or the different mutant lines were detected upon exposure to 8 ºC for one week with respect to 22 ºC (Figure 3A). The analysis of MGDG, DGDG or PG further confirmed the absence of significant changes in the leaf TA content upon exposure to low temperatures, with the exception of PC, in which a decrease of 18:3 was detected in the *fad8i* mutant (Figure 3B and Table S1).

The leaf fatty acid composition from total lipids of Col-0 was not greatly affected by their exposure to 30 ºC (Figure 3A and Table S1). On the contrary, a reduction in TA levels was observed in total lipids from all mutant lines (Figure 3A). Fatty acids from total lipids of *fad7i* showed an important decrease of both 18:3 and 16:3 (down to 13% and 0.5%, respectively; Figure 3A). These values meant an average reduction of 18:3 and 16:3 content of 69.7% and 94%, respectively, when compared with Col-0 (Figure 3A). This reduction of TA levels in *fad7i* at 30 ºC was more pronounced with respect to that detected for the same line at 22 ºC (Figure 3A). A reduction of TA in the *fad8i* mutant was also detected at 30 ºC. As shown in Figure 3A, 18:3 and 16:3 decreased to 28.8% and 4.5%, respectively. These results represented a 26% and 51% reduction for 18:3 and 16:3, respectively, when compared with Col-0 at the same temperature. These data indicated that *fad7i* was more affected than *fad8i* at 30 ºC. A similar conclusion could be drawn from the analysis of the fatty acid composition of individual lipid classes. The 18:3 content in MGDG showed no significant modification upon exposure of Col-0 plants to 30 ºC when compared with the same line at 22 ºC (Figure 3B). In contrast, the 16:3 content in MGDG was more affected, with a 6% decrease when compared with Col-0 at 22 ºC. The TA content of the MGDG from the *fad7i* mutant showed a strong decrease of 18:3 and 16:3 upon exposure to 30 ºC down to 10.5% and 0.6%, respectively (Figure 3B). These values meant an average reduction of 66% and 86.4% in the 18:3 and 16:3 content of MGDG, respectively, with respect to the same line grown at 22 ºC (Figure 3B). In *fad8i*, 18:3 and 16:3 decreased down to 40.8% and 13.7%, respectively (Figure 3B). These values represented an average reduction of 25.8% and 42.9% in the 18:3 and 16:3 content, respectively, with respect to the same line at 22 ºC (Figure 3B). These data suggested that FAD8 activity on MGDG

substrates was more affected by the exposure to 30 ºC than the FAD7 one. This conclusion could be extended to other lipids like DGDG, PC or sulphoquinovosyldiacylglycerol (SQ) (Figure 3B and Table S1). The *fad7 fad8* double mutant also showed a decrease in 18:3 content of MGDG, indicating that FAD3 activity had any or little effect at high temperatures on the fatty acid composition of MGDG (Figure 3B). Finally, the amount of TA in PG decreased in all plants analyzed compared to 22 ºC including Col-0, where a decrease from 27.3% to 14.8% was detected (Figure 3B). In *fad7i* and *fad8i,* 18:3 strongly decreased (down to 3.9% and 5.4%, respectively) to levels very similar to those from the *fad7 fad8* double mutant (2%) (Figure 3B).

Effect of temperature on the expression of the ω-3 fatty acid desaturase genes in the Arabidopsis mutants

We decided to correlate the differences found in the fatty acid composition of the different mutant lines with the expression of the *AtFAD3*, *AtFAD7* and *AtFAD8* genes. q-PCR expression analysis of these genes in leaves from Col-0 and mutant plants grown at 22 ºC or upon exposure for one week to 8 ºC or 30 ºC are shown in Figure 4. Since the triple mutant did not accumulate TAs, the expression analysis was focused in those plant lines where changes in TAs were detected. At 22 ºC, transcripts from *AtFAD3*, *AtFAD7* and *AtFAD8* genes were detected in leaves from four-week old Col-0 plants. The T-DNA insertion provoked the absence of the *AtFAD8* mRNA in the *fad8i* mutant (Figure 4). Very small amounts of the *AtFAD7* mRNA were detected in the *fad7i* mutant in the q-PCR analysis. This small amount of *AtFAD7* mRNA might represent truncated forms of the transcript that are detected in the q-PCR analysis since the primers were designed in the N-terminal region of the protein. This was done to avoid cross-amplification with the highly homologous *AtFAD8* gene. Disruption of the *AtFAD7* and *AtFAD8* genes in the insertion mutants did not result in significant changes in the transcript levels of the *AtFAD8* and *AtFAD7* genes, respectively (Figure 4A). Similarly, the disruption of one or both *AtFAD7* and *AtFAD8* genes did not modify the transcript levels of the ER ω-3 desaturase *FAD3* (Figure 4A). Interestingly, this absence of compensatory responses at the transcriptional level was also observed when the expression of the genes encoding ω-3 fatty acid desaturases was analyzed at either low (8 ºC) or high (30 ºC) temperatures.

Then, we focused our analysis on the Col-0 line where the three *AtFAD3*, *AtFAD7* and *AtFAD8* genes were normally expressed. Col-0 plants exposed to 8 ºC for a week showed a 2-fold increase of *AtFAD8* mRNA when compared to control (22 ºC) plants (Figure 4B). This increase was accompanied by a reduction of the *AtFAD7* transcript levels at low temperatures. These changes in *AtFAD7* and *AtFAD8* transcripts detected at 8 ºC were not accompanied by changes in *AtFAD3* mRNA (Figure 4B). On the other hand, Col-0 plants exposed to 30 ºC showed a significant ($p < 0.05$) decrease of the *AtFAD8* transcript with respect to control (22 ºC) plants (Figure 4B). This could be consistent with the higher sensitivity of FAD8 activity at 30 ºC, (Figures 2 and 3).

Sub-cellular localization of the FAD8 protein

The presence of a chloroplast transit peptide in the *AtFAD8* gene sequence suggested that the FAD8 protein might be located in the plastid (Gibson *et al.*, 1994). To investigate FAD8 function at the protein level, we first analyzed its sub-cellular localization generating stable transgenic Arabidopsis lines expressing the *AtFAD8* gene fused to YFP at its C-terminus, under the control of a constitutive 35S promoter. Transgenic lines generated with the 35S:*FAD8-YFP* construct showed a strong YFP fluorescence signal associated with chloroplasts from leaves (Figure 5B) that was absent in leaves from plants carrying the empty pEarley101 vector (Figure 5A). This YFP signal was found in chloroplasts from mesophyll cells (Figures 5 B, C and F) as well as in the small chloroplasts from guard cells (Figures 5D-E). The YFP signal was not uniform but detected at specific spots or *foci* on the chloroplast (Figures 5B-F). To confirm these results, we performed transient expression experiments in *Nicotiana benthamiana* leaves. The transiently expressed FAD8-YFP protein showed an abundant fluorescent signal associated with plastids (Figures 5 H and I), further corroborating the plastidial localization of FAD8. The signal showed the same pattern of accumulation in *foci* as occurred in the stable transgenic lines (Figures 5 H and I). A similar pattern in small dots on the surface of the chloroplast was also obtained when GFP or CFP were used instead of YFP, suggesting that the pattern observed for FAD8-YFP was not due to the nature of the fluorescent tag (Figure S1). This pattern of localization in discrete foci is shared with many other proteins localized in the plastid, and more concretely in the plastid envelope, expressed under the control of either constitutive or endogenous promoters (Haswell and Meyerowitz, 2006; Maple *et al.*, 2007; Burch-Smith *et al.*,

2011; Ruppel *et al.*, 2011; Yang *et al.*, 2011). To analyze this into detail, Tic40 was used as a control of envelope localization. Tic40 is a component of the TIC translocon and is localized in the inner envelope membrane of the chloroplast (Singh *et al.,* 2008). It has been previously used as a tool for *in vivo* chloroplast envelope localizations (Breuers *et al.,* 2012). Tic40-GFP was transiently expressed in *N. benthamiana* leaves. As shown in Figures 5 J and K, we obtained green small dots structures associated with the chloroplast autofluorescence. This pattern was similar to that reported by Breuers *et al.,* (2012) for the same protein and to that obtained for our 35S:FAD8-YFP construct, supporting the envelope localization of FAD8.

To further confirm the plastidial localization of the FAD8 protein, biochemical fractionation of chloroplasts was carried out, followed by immunoblotting with an anti-GFP antibody that also recognizes the YFP protein. Chloroplasts from leaves of three week-old Arabidopsis plants grown at 22 ºC, carrying both the empty vector and the FAD8-YFP construct, were analyzed. A strong band at the appropriate molecular weight for the FAD8-YFP fusion protein (79-72 kDa) was detected in the transgenic extracts while no signal was observed in plants carrying the empty vector (Figure 6A). Minor bands around 27-30 kDa could also be detected, probably corresponding to processed YFP protein.

The resolution of the confocal microscope cannot inform us about the precise localization of the FAD8 protein within the different chloroplast sub-compartments. Then, the sub-chloroplast membrane distribution of the FAD8-YFP protein was sought. To that end, plants were grown for three weeks under short light period conditions, to favor rosette leaf formation, and intact chloroplasts were isolated through percoll-gradient centrifugation (Bals and Schuneman, 2011). Intact chloroplasts were lysed and envelope, stroma and thylakoid fractions were separated through sucrose gradient centrifugation (Bals and Schuneman, 2011). Fractions were blotted using an anti-GFP antibody to detect the FAD8-YFP protein. Several antibodies were used as specific markers of the different chloroplast sub-fractions. Tic 40, RubisCo and Photosystem II D1 subunit were used as markers of the envelope, stroma and thylakoid, respectively. The results are shown in Figure 6B. The FAD8-YFP protein was detected in the envelope fraction with no detection in the soluble stroma fraction or in the thylakoid membrane. The FAD8-YFP protein distribution was similar to that of Tic 40, the envelope marker, indicating that FAD8-YFP was located in the plastid envelope.

At this point we analyzed whether both plastidial ω-3 desaturases, FAD8 and FAD7, showed similar or different localization patterns in the plastid. To that end, we performed transient expression experiments in *N. benthamiana* leaves in which a 35S:FAD8-CFP construct was co-transformed with a 35S:FAD7-YFP construct. As shown in Figure 7, the FAD7-YFP signal was also detected in small dots or *foci* in the surface of the chloroplasts from *N. benthamiana* (Figure 7A and F), showing a similar accumulation pattern to that observed for FAD8-CFP (Figure 7B and G) or FAD8-YFP (Figure 5). These results suggested that both FAD7 and FAD8 ω-3 desaturases showed a similar pattern of localization in the plastid envelope. Special care was taken to confirm that no YFP signal was detected through the CFP channel or *vice versa* under our experimental conditions. Interestingly, when both FAD7-YFP and FAD8-CFP signals were merged, many of the spots seemed to overlap (Fig. 7D and H), suggesting that both FAD7 and FAD8 desaturases could be located in close vicinity within the membrane.

Over-expression of FAD8 increased 18:3 levels in phospholipids but not in galactolipids.

To gain further insight into the function of the FAD8 protein, the fatty acid composition from total lipids was analyzed in the previously characterized FAD8-YFP over-expressing Arabidopsis lines in which the FAD8 protein was located in the plastid envelope. As shown in Figure 8A, total lipids from different FAD8 over-expressing lines showed an 8-10% increase in 18:3 levels when compared to the plants expressing the empty vector. Interestingly, no modification in 16:3 fatty acids was observed (Figure 8A). This result might be consistent with the data obtained from the analysis of the insertion lines that suggested that FAD8 might be more specific on 18:2 rather than on 16:2 substrates (Figure 2).

The effect on lipid classes of the over-expression of the *AtFAD8* gene was also studied. The transgenic event with the highest increase in 18:3 was further analyzed. No changes in the 18:3 or 16:3 content from the galactolipids MGDG or DGDG was observed in the FAD8 over-expressing lines, further confirming the results obtained in the insertion mutants (Figure 8B). Different results were obtained when the phospholipids were analyzed. As shown in Figure 8B, PG showed a 4-5% increase in 18:3 levels in the FAD8 over-expressing plants. This increase was concomitant with the

decrease of 18:2, indicating a higher ω-3 desaturase activity. Surprisingly, a lipid like PC, mainly present in the ER, also showed an increase in 18:3 levels in the FAD8 over-expressing lines when compared with the plants carrying the empty vector (Figure 8B). This increase (8-10%) was again accompanied by a decrease in 18:2 levels. This increase in 18:3 in extraplastidic lipids was also observed in other lipids like PE or PI (data not shown). Finally, sulpholipids (SQ) also showed a small (5%) but significant ($p<0.1$) increase in 18:3 in the FAD8 over-expressing lines.

DISCUSSION

FAD8 was originally identified as a cold-specific desaturase by the phenotypic analysis of a *fad7* mutation in which the reduction of TA levels observed at control growth temperatures (22 ºC) was less pronounced at low (15 ºC) temperatures (McConn *et al.*, 1994). It was assumed that the role of FAD8 at control temperatures was largely irrelevant. Since then, the study of FAD8 function in plants has been mostly limited to the analysis of the expression profiles of the *FAD8* gene in response to temperature (Berberich *et al.*, 1998; Wang *et al.*, 2006; Martz *et al.*, 2006; Tang *et al.*, 2007; Torres-Franklin *et al.*, 2009; Román *et al.*, 2012). However, some of the functional characteristics of the FAD8 enzyme like its acyl-group chain length and lipid head group specificities or its actual contribution to lipid unsaturation at different temperatures are still poorly understood. Our results support the conclusion that the role of the ω-3 desaturase FAD8 is not only restricted to low temperatures but it is also active at control ones. On one hand, the fatty acid composition analysis from total lipids and lipid classes in two *fad7i* and *fad8i* insertion lines and its comparison with those from the Col-0 line and the *fad7 fad8* double and *fad3 fad7 fad8* triple mutant plants grown at 22 ºC showed that FAD8 partially compensated the absence of a functional *AtFAD7* gene at control growth temperatures (Figure 2). On the other hand, the fatty acid composition analysis of our FAD8 over-expressing lines also showed a specific increase of 18:3 levels at 22 ºC (Figure 8). It is worth mentioning that this increase was detected in the presence of a functional FAD7 enzyme, indicating that the loss of FAD7 desaturase activity is not a prerequisite for the detection of FAD8 activity and that both plastidial ω-3 desaturase activities can occur simultaneously, even at control temperatures.

In addition to this, the fatty acid composition analysis on both total lipids and lipid classes in our mutants revealed two interesting features of FAD8 that suggest that its role might not be redundant with respect to FAD7. First, FAD8 activity always increased 18:3 levels without changes in 16:3 ones. These results were obtained either in the compared analysis of the *fad7i*, *fad8i*, double *fad7 fad8* and triple *fad3 fad7 fad8* mutants (Figure 2) or the FAD8 over-expressing lines (Figure 7), suggesting that FAD8 might have a higher selectivity for 18:2 acyl-lipid substrates rather than for 16:2 ones. Moreover, our lipid class analysis suggested that FAD8 exhibited a higher preference for lipids other than galactolipids, especially PG, in contrast to what happened with

FAD7 that showed a higher preference for MGDG and DGDG, (Horiguchi et al., 1996; Kodama et al., 1995). PG is the only phospholipid detected in thylakoids (Joyard *et al.*, 1998) and lacks 16:3, 18:3 being the only TA species esterified to PG at the *sn-1* position. Although it only represents an 8-10% from total lipids, its role on the arrangement of photosynthetic complexes, thylakoid membrane formation, chilling sensitivity and low-temperature adaptation has been well established (Hagio *et al.*, 2002; Sakamoto *et al.*, 2004; Wada and Murata, 2007). These results altogether suggest that although similar in sub-cellular localization, the function and roles of FAD7 and FAD8 may not be redundant. While FAD7 would be responsible for the unsaturation of 16:2 and 18:2 with higher preference for the major leaf lipids MGDG and DGDG, constituting the bulk lipid fraction of chloroplast membrane, FAD8 would be highly specific for 18:2 substrates with preference for other minor lipid classes like PG, with relevant roles in chloroplast dynamics. The differences in the amount of these lipids in the leaf cell (MGDG and DGDG can represent an almost 80% of total leaf lipids while PG can reach an 8%) may also explain why the compensatory effect of the FAD7 ω-3 desaturase activity in the *fad8* mutant was almost complete while the compensatory effect of the FAD8 ω-3 desaturase activity in the *fad7* mutant was only partial. The differences found between FAD8 and FAD7 ω-3 desaturase activity in the use of acyl-lipid substrates are particularly relevant if we have in mind that fatty acid desaturases catalyze highly selective reactions (Behrouzian and Buist, 2002). An attractive hypothesis explaining this higher selectivity of FAD8 for 18:2 substrates could be that FAD8 acts preferentially on fatty acids esterified to *sn*-1 position of glycerolipids. This might explain why FAD8 acts poorly on 16:2 substrates (always in *sn*-2 position) or the higher selectivity for PG (that contains 18:2 only in *sn*-1).

The fatty acid composition analysis of the *fad7i* and *fad8i* mutants showed compensatory responses at the TA level as a result of the inactivation of the *FAD7* and *FAD8* genes, respectively. However, our q-PCR analysis indicated that these compensatory responses of the ω-3 desaturase activity did not result from compensatory transcriptional responses acting on the desaturase genes. Similarly, the disruption of one or both *AtFAD7* and *AtFAD8* genes did not modify the transcript levels of the endoplasmic reticulum ω-3 desaturase FAD3 (Figure 4A), suggesting that the compensatory responses were controlled at the post-transcriptional level. However, our q-PCR data showed an increase in *AtFAD8* transcript levels upon exposure to 8 ºC that

was concomitant to a decrease of *AtFAD7* mRNA (Figure 4). These results are consistent with those previously reported in maize (Berberich *et al.,* 1998), birch (Martz *et al.,* 2006), rice (Wang *et al.,* 2006), or *Descurainia sophia* (Tang *et al.,* 2007), suggesting that transcriptional control participates in the regulation of FAD8 activity and the coordination among plastidial desaturases, at least in response to low temperatures. Unfortunately, there are no specific antibodies against the *At*FAD8 or *At*FAD7 proteins that might provide information about the relative abundance of these enzymes and how these transcriptional and post-transcriptional control mechanisms work to maintain an appropriate unsaturation level of membrane glycerolipids. Differently to what happens with the endoplasmic reticulum ω-3 desaturase FAD3, plastid fatty acid desaturases are almost impossible to assay either *in vivo* or *in vitro*. They have specific requirements for their activity such as reduced ferredoxin and $NADPH_2$ generated in the plastid. Accordingly, only if located in the correct plastid membrane environment, in the presence of its natural cofactors, would FAD8 show ω-3 desaturase activity. Data from our stable transgenic lines over-expressing a FAD8-YFP protein as well as our transient expression experiments in *N. benthamiana* confirmed the plastidial localization of FAD8 desaturase. The biochemical fractionation of chloroplasts from our FAD8 over-expressing lines showed that the FAD8 protein was present in the envelope membrane of chloroplasts. This localization confirmed previous proteomic data (Froehlich *et al.,* 2003), indicating that the pattern of localization of the FAD8 protein was genuine and not due to the ectopic expression of the protein. In addition to this, our data from FAD8 over-expressing lines showed an increase of ω-3 desaturase activity acting specifically on 18:2 fatty acids from lipids other than galactolipids, confirming the results obtained with the mutants. Over-expression of the *AtFAD7* gene in tobacco plants resulted in an increase of both 18:3 and 16:3 levels (Kodama *et al.,* 1995), further supporting our conclusion of the higher specificity of FAD8 for 18:2 acyl-lipid substrates. It is worth mentioning the effect of the over-expression of plastidial FAD8 on extraplastidial lipids like PC. Similar effects on extraplastidial lipids due to the over-expression of plastidial desaturases have been reported in the case of *At*FAD7 in *Nicotiana* (Kodama *et al.,* 1995) and more recently in *Chlamydomonas* (Nguyen *et al.,* 2013). They could be probably due to the transfer of ω-3 acyl-chains from plastidial to extraplastidial membranes. Such an export of 18:3 into extraplastidial membranes was first discovered in Arabidopsis mutants deficient in fatty acid unsaturation (Miquel and Browse, 1992; Browse *et al.,* 1993). However, other

possibilities like mistargeting of a portion of the over-expressed protein to the ER cannot be precluded. It has been demonstrated that re-targeting of the plastidial FAD4 desaturase to the cytoplasm, resulted in a change of the regiospecificity (Δ^7 to Δ^6) of the enzyme (Heilmann et al., 2004).

In the absence of an appropriate mean to perform specific activity assays that might help us to establish the enzymatic properties of each plastidial ω-3 desaturase, both the biochemical evidences showing the envelope localization of the FAD8 protein together with the specific ω-3 desaturase activity producing 18:3 in lipids other than galactolipids provide experimental evidence of the non-redundant role of FAD8 in the plant glycerolipid unsaturation pathway. Despite this non-redundant role, our results indicate that in Arabidopsis, both FAD8 and FAD7 ω-3 desaturases are located in the plastid envelope membrane. Question arises how these proteins are organized in the membrane and how this organization is relevant to their function. Our present knowledge of the supramolecular organization of plant fatty acid desaturases and their distribution in the chloroplast membranes is very limited. Our co-localization experiments suggest a close spatial relationship between both enzymes. These results open the way to analyze the degree of interaction and distribution of both FAD7 and FAD8 plastidial ω-3 desaturases, as well as the ω-6 desaturase FAD6 in the envelope to maintain a proper functioning of the sequential desaturation pathway.

METHODS

Plant materials and experimental treatments

The lines of *Arabidopsis thaliana* used were descended from the Columbia 0 ecotype (Col-0). Two insertional mutants from SALK were used: *fad7i* (SALK_147096C) and *fad8i* (SALK_093590). These insertion lines were selected after discarding other plant lines carrying insertions in loci other than *AtFAD8* (*At5g05570*). We also used a double *fad7-1 fad8-1* mutant from NASC (NASC N8036) and a triple mutant (*fad3-2 fad7-2 fad8-1*), a kind gift from Prof. John Browse (Washington State University, Pullman, WA USA). All plants were grown on soil in a bioclimatic chamber under a light intensity of 120-150 μmol^{-2} s^{-1}, with a 16h/8h light/darkness photoperiod at 22 ºC and a relative humidity of 45%. After three weeks of growth, plants were kept at 22 ºC (control treatment), or transferred to 30 ºC (high-temperature treatment) or 8 ºC (low-temperature treatment) for an additional week. Three pools of rosette leaves from each plant line were collected at the end of the treatment, frozen in liquid nitrogen and stored at -80 ºC until use.

Molecular characterization of the insertion lines

PCR on genomic DNA was performed using the primer LB (5'-TGGTTCACGTAGTGGGCCATCG-3', http://signal.salk.edu/tdnaprimers.html) or the RB primer 5'- GTCATAACGTGACTCCCTTAATTCTCC-3') in combination with the *AtFAD7* (7F, 5'- CAAGTTCTAATGGCGAACTTGGTCTTA-3' and 7R, 5'-CAAGCCTGCTTCATTTCAATCTGCTCT-3') and *AtFAD8* (8F, 5'-CTTGGGAAGAGGCTCCAAT-3' and 8R, 5'-GTAACTTGTCTGCCTGGTTCAC-3') gene specific primers. A PCR of the entire gene was also performed with the *AtFAD7* and *AtFAD8* primers to check the homozygosis of the mutations. The presence of a pROK vector fragment used to generate SALK lines was confirmed by sequencing (CNIO, Madrid, Spain). The *AtFAD3*, *AtFAD7* and *AtFAD8* genes from the double *fad7 fad8* and triple *fad3 fad7 fad8* mutants were also sequenced to analyze the mutations in the corresponding genes.

Lipid analysis

Total lipids were extracted from 0.5 g rosette leaves as described (Bligh and Dyer, 1959). Individual lipids were purified by two-dimensional thin-layer chromatography (TLC), according to Hernández *et al.,* (2008). Fatty acid methyl esters of total lipids or individual lipid classes were produced by acid-catalyzed transmethylation (Garcés and Mancha, 1993) and analyzed by gas chromatography (GC), using a 7890A (Agilent, Santa Clara, CA USA) fitted with a capillary column (30-m length; 0.32-mm inner diameter; 0.2-µm film thickness) of fused silica (Supelco, Bellafonte, PA, USA) and a FID detector. 17:0 was used as internal standard. Hydrogen was used as a carrier gas with a linear rate of 1.34 ml min^{-1} and split ratio of 1/50. The injector and detector temperature was 220 °C and the oven temperature was 170 °C. Data from fatty acid analysis were obtained from three independent biological experiments with two technical repeats for experiment. Analysis of variance (ANOVA) was applied to compare treatments. Statistical analyses were carried out with the program Statgraphics Plus for Windows 2.1, using a level of significance of 0.05.

Expression analysis of the desaturase genes

Total RNA was isolated from 0.1 g of rosette leave tissues with Trizol (Life Technologies) and first-strand cDNA was synthesized from 3 µg total RNA with M-MLV reverse transcriptase (Promega) and oligo dT. Quantitative PCR (q-PCR) was performed using a 7500 Real Time PCR System (Applied Biosystems) and SYBR Green Master Mix (Applied Biosystems). The gene expression levels were calculated relative to EF1α reference gene (*At5g60390*) using the $2^{-\Delta\Delta Ct}$ method (Livak and Schmittgen, 2001). The oligonucleotides used were: q*AtFAD3F*, 5'-CGCCACGAAAGCAGCTAAAC-3' and q*AtFAD3R*, 5'-TCGGTATTGCTCCTGACGTCTT-3'; q*AtFAD7F*, 5'-CTCTCCAACAACAACAAATTCAGAC-3' and q*AtFAD7R*, 5'-CCAAAAGACAGAGGAGATGATGAT-3'; q*AtFAD8F*, 5'-GCCTCTAACCCTAAACCCA-3' and q*AtFAD8R*, 5'-CGGGAATTGAGAAGAGAAGAA-3'; *qEF1-αF*, 5'-TGAGCACGCTCTTCTTGCTTTCA-3', and *qEF1-αR*, 5'-GGTGGTGGCATCCATCTTGTTACA-3'. Data were obtained from the analysis of

three independent biological experiments with at least three technical repeats for experiment.

Generation of transgenic Arabidopsis lines

The *AtFAD8* (At5g05580) coding sequence was PCR-amplified using the specific primers 5'-CACCATGGCGAGCTCGGTTTTAT-3' and 5'-GGCTGTTCTTTGTCCATTGAGTTTTGGAT-3' and cloned in the pENTER-TOPO® vector. The forward primers include CACC for TOPO cloning, and the reverse primers have been modified to change the stop codon to alanine. PCR reactions were performed with Phusion High-fidelity DNA polymerase (Thermo Scientific) according to manufacturer's instructions. pENTR vector construction was also performed according to manufacturer's instructions (Invitrogen) and used for *E.coli* DH5α transformation. The *AtFAD8* gene, now flanked by the appropriate AttL sites, was sub-cloned into the GATEWAY®-compatible binary vector pEarleyGate101 fused to the YFP at the C-terminus under the control of a 35S constitutive promoter (Earley *et al.,* 2006). Construction of destination vectors was performed using Gateway LR clonase II enzyme mix (Invitrogen). The resulting construct and the empty vector used as negative control were introduced into *Agrobacterium tumefaciens* (strain GV3101 pMP90) by electroporation. Selection media in *E. coli* was kanamycin and in *A.tumefaciens* were gentamycin + kanamycin. Sequencing and colony-PCR were performed at all stages to ensure correct sequence and alignment.

Arabidopsis plants were transformed with *A. tumefaciens* harbouring the constructs FAD8-YFP and pEarlyGate101 as negative control by the simplified floral dip method (Clough and Bent, 1998). Seeds were collected and selected in MS plates supplemented with the glufosinate-ammonium herbicide. After three generations, only homozygous plants were selected. For the experiments with the transgenic lines, two different transgenic homozygous events (1.13 and 3.1) were analyzed.

Transient expression in *Nicotiana benthamiana*

Different constructs were used for transient expression experiments in *Nicotiana benthamiana* leaves. In addition to the 35S:FAD8-YFP construct used for the generation of the stable FAD8 overexpressing lines, TIC40 (At5g16620) that encodes a component of the TIC (Translocon of the inner chloroplast membrane complex) was

used as an inner envelope membrane marker for localization studies. Specific primers for Tic40, Tic40F, 5'- CACCATGGAGAACCTTACCCTAGTTTCT-3' and Tic40R, 5'- GGCACCCGTCATTCCTGGGAAC-3' were used for amplification of the *TIC40* gene and cloned in the pENTER-TOPO® vector. In this case, the pMDC83 vector (Curtis and Grossniklaus, 2003) that carries a 35S constitutive promoter and GFP as C-terminal fluorescent tag were used for localization analysis. A 35S:FAD8-GFP was also generated from the cloned *AtFAD8* gene and pMDC83 vector as described above. For co-localization purposes, two additional constructs were also generated. The *AtFAD7* gene (At3g11170) was amplified with specific primers AtFAD7F: 5'-CACCATGGCGAACTTGGTCTTATC-3' and AtFAD7R: 5'-GGCATCTGCTCTTACTTTGACCTCTC-3', and cloned in the pENTER-TOPO® vector. pEarley 101 was used as destination vector to generate a 35S:FAD7-YFP construct. A second 35S:FAD8-CFP construct was also generated using pEarley 102 as destination vector.

N. benthamiana leaves from 5-week old plants, grown at 22 ºC, 16 h light, 8 h dark photo period were infiltrated with *A. tumefaciens* cultures (OD_{600nm} 0.5), harbouring either FAD8-YFP, FAD8-GFP, FAD8-CFP, Tic40-GFP or the empty vectors (pEarley101, pEarley102 or pMDC83). All constructs were co-infiltrated with the p19 plasmid to avoid silencing (Voinnet et al, 2003), according to Hernández *et al.*, (2012). For co-localization experiments, a combination of *A. tumefaciens* cultures (OD_{600nm} 0.5), carrying either the FAD7-YFP or the FAD8-CFP contructs were used. Plants were kept in the growth chamber for another 3-5 days before analysis.

Confocal microscopy analysis

Fresh leaf imaging was carried out on a Leica TCS SP II confocal microscope. Images were acquired using a 40x, 63x or 100x oil immersion objectives. Imaging of GFP, YFP and CFP emissions were performed by sequential scanning. GFP, YFP and CFP were excited with the 488, 514 and 458 nm lines, respectively, of an argon laser and the emission collected through a 505-560 nm emission filter for GFP, 518-580 nm emission filter for YFP and 465-571 nm for CFP. Autofluorescence of chlorophyll was excited with the 633 nm line of an argon laser, and the emission was collected through a 651-717 nm emission filter. Images were taken with 6-8 line averaging. Images were analyzed and merged using Leica AF and Image J software.

Sub-cellular fractionation and immunoblot analysis

Protein extracts were obtained from 0.5 g of Arabidopsis rosette leaves crushed in a mortar with liquid nitrogen. The powder was then dispersed in buffer A (0.1 M TRIS-HCl, pH: 7.5, 20% (w/v) glycerol, 1 mM EDTA, 10 mM $MgCl_2$, 14 mM β-mercaptoethanol, 100 µg/ml Pefabloc (Fluka), 1 µg/ml antipain (Sigma-Aldrich) and 1 µg/ml leupeptin, (Sigma-Aldrich) and filtered through a layer of Miracloth paper (Calbiochem). Chloroplasts and further sub-chloroplast fractionation into thylakoid, stroma and envelope fractions was performed as described in Bals and Schünemann (2011). Protein content of the different fractions was estimated using the BioRad protein assay reagent. Total protein of 10 µg was loaded per lane. Western blot procedures were performed as described in Andreu et al. (2010) using the commercial antibodies against GFP (ab290, Abcam) or Tic40, RuBisCO and D1 (Agrisera) as protein markers of the envelope, stroma and thylakoid fractions, respectively. Antibody dilutions were 1:2000 for Tic40 and D1 and 1:10.000 for RuBisCo. Detection was carried out using a highly sensitive chamiluminiscent reagent for peroxidase detection (SuperSignal West Pico, Pierce).

SUPPLEMENTARY DATA

Table S1. Effect of temperature on the fatty acid composition from lipid classes isolated from the different plant lines used in this study.

Figure S1. Confocal microscopy localization of FAD8-GFP and FAD8-CFP in *Nicotiana benthamiana* leaves.

FUNDING

This work was supported by the Spanish Ministry of Economy and Competitiveness (MINECO), (AGL2011-23574, AGL2011-24442 and AGL2014-55300-R) and Aragón Government (Grant E33). A.R. and B.L. were recipient of a predoctoral fellowship from JAE-Pre (CSIC) and A.S. from the FPI (MINECO) Programs. M.L. Hernández and S. López-Gomollón had a postdoctoral contract from the JAE-Doc Program (CSIC).

Individual Author's contribution:

A.R. conducted most part of the experimental work; M-L.H. contributed to the lipid analysis; A. S.-G. performed the qPCR expression analysis; S. L.-G. performed the co-localization studies; B.L. contributed with the FAD7-YFP construct; R.P. participated in the design of the experiments and in the discussion of the data; J.M. M.-R, provided expertise in the lipid analysis, and in the design of the experiments and discussion of the results; M.A. contributed with the results using the GFP tag, designed the experiments, supervised the work and wrote the manuscript.

ACKNOWLEDGEMENTS

Authors wish to thank Dr. Victoria López (EEAD-CSIC) for help in the statistical analysis of the data and David Velázquez (IG-CSIC) for help in transient expression analysis.

REFERENCES

Andreu, V., Collados, R., Testillano, P.S., Risueño, M.C., Picorel, R., and Alfonso, M. (2007). In situ molecular identification of the plastid ω-3 fatty-acid desaturase FAD7 from soybean:evidence of thylakoid membrane localization. Plant Phys. **145**, 1336-1344.

Andreu, V., Lagunas, B., Collados, R., Picorel, R., and Alfonso, M. (2010). The *GmFAD7* gene family from soybean: identification of novel genes and tissue-specific conformations of the FAD7 enzyme envolved in desaturase activity. J. Exp. Bot. **61**, 3371-3384.

Bals, T., and Schünemann, D. (2011). Isolation of Arabidopsis thylakoid membranes and their use for *in vitro* protein insertion or transport assays. Methods in Mol. Biol. **774**, 321-338.

Behrouzian, B., and Buist, P.H. (2002). Fatty acid desaturation: variations on an oxidative theme. Curr. Op. Chem. Biol. **6**, 577-582.

Berberich, T., Harada, M., Sugawara, K., Kodama, H., Iba, K., and Kusano, T. (1998). Two maize genes encoding ω-3 fatty-acid desaturase and their differential expression to temperature. Plant Mol. Biol. **36**, 297-306.

Bilyeu, K.D., Palavalli, L., Sleper, D.A., and Beuselinck, P.R. (2003). Three microsomal desaturase genes contribute to soybean linolenic acid levels. Crop Sci. **43**, 1833-1838.

Bligh, E.G., and Dyer, W.S. (1959). A rapid method of total lipid extraction and purification. Can. J. Biochem. Physiol. **37**, 911-917.

Breuers, F.K.H., Bräutigam, A., Geimer, S., Welzel, U.Y., Stefano, G., Renna, L., Brandizzi, F., and Weber, A.P.M. (2012) Dynamic remodelling of the plastid envelope membranes – atool for chloroplast envelope invivo localizations. Front. Plant Sci. **3**, 1-10.

Browse, J., McCourt, P., and Somerville, C. (1986). A mutant of *Arabidopsis* deficient in C(18:3) and C(16:3) leaf lipids. Plant Physiol. **81**, 859-864.

Browse, J., and Somerville, C. (1991). Glycerolipid synthesis: Biochemistry and regulation. Ann. Rev. Plant Physiol. **42**, 467-506.

Browse, J., McConn, M., James, D., and Miquel, M. (1993). Mutants of Arabidopsis deficient in the synthesis of α-linolenate. J. Biol. Chem. **268**, 16345-16351.

Burch-Smith, T.M., Brunkard, J.O., Choi, Y.G., and Zambruski, P.C. (2011). Organelle-nucleus cross-talk regulates plant intercellular communication via plasmodesmata. Proc. Natl. Acad. Sci. USA **108**, 1451-1460.

Clough, S.J., and Bent, A.F. (1998). Floral dip: a simplified method for Agrobacterium-mediated transformation of *Arabidopsis thaliana*. Plant J. **16**, 735–743.

Curtis, M. and Grossniklaus, U. (2003). A Gateway™ cloning vector set for high-throughput functional analysis of genes in plants. Plant Physiol. **133**, 462-469.

Dyer, J.M., and Mullen, R.T. (2001). Immunocytological localization of two plant fatty acid desaturases in the endoplasmic reticulum. FEBS Lett. **494**, 44-47.

Earley, K.W., Haag, R., Pontes, O., Opper, K., and Juehne, T. (2006). Gateway-compatible vectors for plant functional genomics and proteomics. Plant J. **45**, 616-629.

Froehlich, J.E., Wilkerson, C.G., Ray, K.G., McAndrew, R.S., Osteryoung, K.W., Gage, D.A., and Phinney, B.S. (2003). Proteomic study of the Arabidopsis thaliana chloroplastic envelope membrane utilizing alternatives to traditional two-dimensional electrophoresis. J. Proteome Res. **2**, 413-425.

Garcés, R., and Mancha, M.. (1993). One-step lipid extraction and fatty acid methyl esters preparation from fresh plant tissues. Anal. Biochem. **211**, 139-143.

Gibson, S., Arondel, V., Iba, K., and Somerville, C. (1994). Cloning of a temperature-regulated gene encoding a chloroplast w-3 desaturase from *Arabidopsis thaliana*. Plant Physiol. **106**, 1615-1621.

Hagio, M., Sakurai, I., Sato, S., Kato, T., Tabata, S., and Wada, H. (2002). Phosphatidylglycerol is essential for the development of thylakoid membranes in *Arabidopsis* thaliana. Plant Cell Physiol. **43**, 1456-1464.

Haswell, E.S., and Meyerowitz, E.M. (2006). MscS-like proteins control plastid size and shape in *Arabidopsis thaliana*. Curr. Biol. **16**, 1-11.

Heilmann, I., **Pidkowich, M.S., Girke, T., and Shanklin, J.** (2004). Switching desaturase enzyme specificity by alternate subcellular targeting. Proc. Natl. Acad. Sci. USA **101**, 10266-10271.

Hernández, M.L., Guschina, I.A., Martínez-Rivas, J.M., Mancha, M., and Harwood, J.L. (2008). The utilization and desaturation of oleate and linoleate during glycerolipid biosynthesis in olive (*Olea europea* L.) callus cultures. J. Exp. Bot. **59**, 2425-2435.

Hernández, M.L., Whitehead, L., He, Z., Gazda, V., Gilday, A., Kozhevnikova, E., Vaistij, F.E., Larson, T.R., and Graham, I.A. (2012)**.** A Cytosolic Acyltransferase Contributes to Triacylglycerol Synthesis in Sucrose-Rescued *Arabidopsis* Seed Oil Catabolism Mutants. Plant Physiol. **160**, 215–225.

Horiguchi, G., Kodama, H., Nishimura, M., and Iba, K. (1996). Role of ω-3 fatty-acid desaturases in the regulation of the level of trienoic fatty acids during leaf cell maturation. Planta **199**, 439-442.

Joyard, J., Maréchal, E., Miege, C., Block, M.A., Dorne, A.-J., and Douce, R. (1998). Structure, distribution and biosynthesis of glycerolipids from higher plant chloroplasts. In: Siegenthaler P-A, Murata N (eds) *Lipids in Photosynthesis*. Kluwer AcademicPublishers, Dordrecht, The Netherlands, pp 21-52.

Kodama, H., Horiguchi, G., Nishiuchi, T., Nishimura, M., and Iba, K. (1995). Fatty acid desaturation during chilling acclimation is one of the factors involved in conferring low-temperature tolerance to young tobacco leaves. Plant Physiol. **107**, 1177-1185.

Lagunas, B., Román, A., Andreu, V., Picorel, R., and Alfonso, M. (2013). A temporal regulatory mechanism controls the different contribution of endoplasmic

reticulum and plastidial omega-3 desaturases to trienoic fatty acid content during leaf development in soybean (*Glycine max* cv Volania). Phytochem. **95**, 158-167.

Livak, K.J., and Schmittgen, T.D. (2001). Analysis of relative gene expression data using real-time quantitative PCR and the 2(-Delta Delta C (T)) method. Methods **25**, 402-408.

Maple, J., Votja, L., Soll, J., and Moller, S.G. (2007). *ARC3* is a stromal z-ring accessory protein essential for plastid division. EMBO Rep. **8**, 293-309.

Martz, F., Kiviniemi, S., Plava, T.E., and Satinen, M.L. (2006). Contribution of omega-3 fatty acid desaturase and 3-ketoacyl-ACP synthase II (KASII) genes in the modulation of glycerolipid fatty acid composition during cold acclimation in birch leaves. J. Exp. Bot. **57**, 897-909.

Matsuda, O., Sakamoto, H., Hashimoto, T., and Iba, K. (2005). A temperature-sensitive mechanism that regulates post-translational stability of a plastidial ω-3 fatty-acid desaturase (FAD8) in *Arabidopsis* leaf tissues. J. Biol. Chem. **280**, 3597-3604.

McConn, M., Hugly, S., Browse, J., and Somerville, C. (1994). A mutation at the *fad*8 locus of *Arabidopsis* identifies a second chloroplast ω-3 desaturase. Plant Physiol. **106**, 1609-1614.

McConn, M., and Browse, J. (1996). The critical requirement for linolenic acid is pollen development, not photosynthesis in an Arabidopsis mutant. Plant Cell **8**, 403-416.

Miquel M., and Browse, J. (1992). Arabidopsis mutants deficient in polyunsaturated fatty acid synthesis. J. Biol. Chem. **267**, 1502-1509.

Nguyen, H.M., Cuivé, S., Bylay-Adriano, A., Légeret, B., Billon, E., Auvrey, P., Beisson, F., Peltier, G., and Li-Beisson, Y. (2013). The green alga *Chlamydomonas reinhradtii* has a single ω3 fatty acid desaturase that localizes to the chloroplast and impacts both plastidic and extraplastidial membrane lipids. Plant Physiol. **163**, 914-928.

Ohlrogge, J., and Browse, J. (1995). Lipid biosynthesis. Plant Cell **7**, 957-970.

Román, A., Andreu, V., Hernández, M.L., Lagunas, B., Picorel, R., Martínez-Rivas, J.M., and Alfonso, M. (2012). Contribution of the different omega-3 fatty acid desaturase genes to the cold response in soybean. J. Exp. Bot. **63**, 4973-4982.

Ruppel, N.J., Logsdon, C.A., Whippo, C.W., Inoue, K., and Hangarter, R.P. (2011). A mutation in *Arabidopsis* SEEDLING PLASTID DEVELOPMENT1 affects plastid differentiation in embryo-derived tissues during seedling growth. Plant Physiol. **155**, 342-353.

Sakamoto, A., Sulpice, R., Kaneseki, T., Hou, C.X., Kinoshita, M., Higashi, S., Moon, B.Y., Nonaka, H., and Murata, N. (2004). Genetic modification of fatty acid unsaturation of chloroplastic phosphatidylglycerol alters the sensitivity to cold stress. Plant Cell Environ. **27**, 99-105.

Schmidt, H., and Heinz, E. (1990). Desaturation of oleoyl groups in envelope membranes from spinach chloroplast. Proc. Natl. Acad. Sci. USA **87**, 9477-9480.

Singh, N.D., Li, M., Lee, S.B., Schnell, D., and Daniell, H. (2008). *Arabidopsis* Tic40 expression in tobacco chloroplasts results in massive proliferation of the inner envelope membrane and upregulation of associated proteins. Plant Cell **20**, 3405-3417.

Tang, S., Guan, R., Zhang, H., and Huang, J. (2007). Cloning and expression analysis of three cDNAs encoding omega-3 fatty acid desaturases from *Descurainia sophia*. Biotech. Lett. **29**, 1417-1424.

Torres-Franklin, M.L., Repellin, A., Huynh, V.B., d'Arcy-Lameta, A., and Zuily-Fodil, Y. (2009). Omega-3 fatty acid desaturase (*FAD3*, *FAD7*, *FAD8*) gene expression and linolenic acid content in cowpea leaves submitted to drought and after rehydration. Environ. Exp. Bot. **65**, 162-169.

Voinnet, O., **Rivas, S., Mestre, P., and Baulcombe, D.** (2003). An enhanced transient expression system in plants based on suppression of gene silencing by the p19 protein of tomato bushy stunt virus. Plant J. **33**, 949-956.

Vrinten, P., Hu, Z.Y., Munchinsky, M.A., Rowland, G., and Qiu, X. (2005). Two FAD3 desaturase genes control the level of linolenic acid in flax seed. Plant

Physiol. **139**, 79-87.

Wada, H., and Murata, N. (2007). The essential role of phosphatidylglycerol in photosynthesis. Photosynth. Res. **92**, 205-215.

Wallis, J., and Browse, J. (2002). Mutants of *Arabidopsis* reveal many roles for membrane lipids. Progr. Lipid Res. **41**, 254-278.

Wang, J., Ming, F., Pittman, J., Han, Y., Hu, J., Guo, B., and Shen, D. (2006). Characterization of rice (*Oryza sativa* L.) gene encoding a temperature-dependent chloroplast ω-3 fatty acid desaturase. Biochem. Biophys. Res. Com. **340**, 1209-1216.

Yadav, N.S., Wierzbicki, A., Aegerter, M., Caster, C.S., Pérez-Grau, L., Kinney, A.J., Hitz, W.D., Russell Booth, J., Schweiger, B., Stecca, K.L., Allen, S.M., Blackwell, M., Reiter, R.S., Carlson, T.J., Russell, S.H., Feldmann, K.A., Pierce, J., and Browse, J. (1993). Cloning of higher plant ω3 fatty-acid desaturases. Plant Physiol. **103**, 467-476.

Yang, Y., Sage, T.L., Liu, Y., Ahmas, T.R., Marshall, W.F., Shiu, S.H., Froelich, J.E., Imre, K.M., and Osteryoung, K.W. (2011). CLUMPED CHLOROPLAST1 is required for plastid separation in *Arabidopsis*. Proc. Natl. Acad. Sci. USA **108**, 18530-18535.

FIGURE LEGENDS

Figure 1. **Genotypic characterization of the Arabidopsis insertional mutants *fad8i* (SALK_093590) and *fad7i* (SALK_147096C).** (A) Schematic diagram showing the localization of the T-DNA insertions in the mutants. Exons are shown as white boxes. The triangles are used to mark the insertions. The arrows indicate the primers used for genotyping and expression analysis. (B) Characterization by PCR of the insertions. Left panels (gDNA) and right panels (cDNA) from Col-0, *fad7i* and *fad8i* plants. *ACTIN* was used as a housekeeping gene.

Figure 2. Fatty acid composition of total lipids and lipid classes from Arabidopsis Col-0 and mutant lines at 22 ºC. (A) Fatty acid composition of total lipids from Arabidopsis Col-0 and mutant lines (*fad7i*, *fad8i*, *fad7 fad8* and *fad3 fad7 fad8*) grown at 22 ºC. (B) Trienoic fatty acids content in MGDG, DGDG, PC and PG lipid classes. Data are mean of three biological experiments with two technical repeats for each experiment.

Figure 3. Trienoic fatty acid content of total lipids and lipid classes from Arabidopsis Col-0 and mutant lines grown at 8, 22 and 30 ºC. (A) Trienoic fatty acid composition of total lipids from Arabidopsis Col-0 and mutant lines (*fad7i*, *fad8i*, *fad7 fad8*) grown at 8, 22 and 30 ºC. (B) Trienoic fatty acid content in MGDG, PC and PG from Col-0 and mutant lines. Data are mean of three biological experiments with two technical repeats for each experiment.

Figure 4. Expression of the *AtFAD8*, *AtFAD7* and *AtFAD3* genes from Col-0 and mutant lines at 22, 8 and 30 ºC. (A) q-PCR expression data of the *AtFAD8*, *AtFAD7* and *AtFAD3* genes from Col-0 and *fad7i*, *fad8i*, *fad7 fad8* and *fad3 fad7 fad8* mutants grown at 22, 8 and 30 ºC. Data were calibrated relative to the corresponding gene expression level in Col-0. (B) q-PCR expression data of *AtFAD8*, *AtFAD7* and *AtFAD3* genes from Col-0 plants grown at 22, 8 and 30 ºC. Data were calibrated relative to the corresponding gene expression level at 22 ºC. *EF1-α* was used as a housekeeping gene. Data are mean ± SD of three biological replicates with at least three technical repeats for each experiment.

Figure 5. Expression of *At*FAD8-YFP fusion protein in stable transgenic Arabidopsis lines and transiently in *N. benthamiana* leaves. (A-F) Transgenic Arabidopsis lines: (A) leaves from plant transformed with the pEarley101 empty vector. (B-F) Leaves from plants transformed with FAD8-YFP fusion protein. (B), (C) and (F), mesophyll cells; (D) and (E), guard cells. (G-I), transient expression assay in *N. benthamiana* leaves: (G) plant transformed with the pEarley101 empty vector. (H) and (I) plants transformed with *At*FAD8-YFP fusion protein. (J-K) plants transformed with Tic40-GFP fusion protein as a control for positive envelope localization, (L) plants harbouring the empty pMDC83 vector. Scale bar is 50 μm in pictures A, B, D, F, G, H, J, and L, and 10 μm in pictures C, E, I and K.

Figure 6. Expression and accumulation of the FAD8-YFP fusion protein. (A) Western blot using an anti-GFP antibody in chloroplasts isolated from plants transformed with the empty vector (pE101) and with the 35S:FAD8-YFP construct. Total protein of 10 μg was loaded per lane. (B) Biochemical fractionation of isolated chloroplasts from FAD8-YFP over-expressing lines. Chl, chloroplasts; Env, envelope; Str, stroma, Thyl, thylakoid fractions. Anti-Tic40, anti-RuBisCO and anti-D1 were used as protein markers of the envelope, stroma and thylakoid fractions from chloroplasts.

Figure 7. **Co-localization analysis of FAD8-CFP and FAD7-YFP fusion proteins by transient expression in *N. benthamiana* leaves.** (A and E) FAD7-YFP, (B and F) FAD8-CFP, (C and G) autofluorescence of the chlorophyll from plastids, (D and H) merged image from A,B , C and E, F,G, respectively. Scale bar is 20 μm in all pictures.

Figure 8. Fatty acid composition of total lipids and lipid classes from FAD8-YFP over-expressing lines grown at 22 ºC. (A) Total lipids in lines harbouring the empty pEarleyGate101 vector and F8 1.13 and 3.1 over-expressing the FAD8-YFP protein. (B) 16:3, 18:3 and 18:2 content in MGDG, DGDG, PC and PG. White bars represent plants carrying the empty pE101 vector and black bars F8 3.1 plants over-expressing the FAD8-YFP protein.

Fig. 1. Román et al.

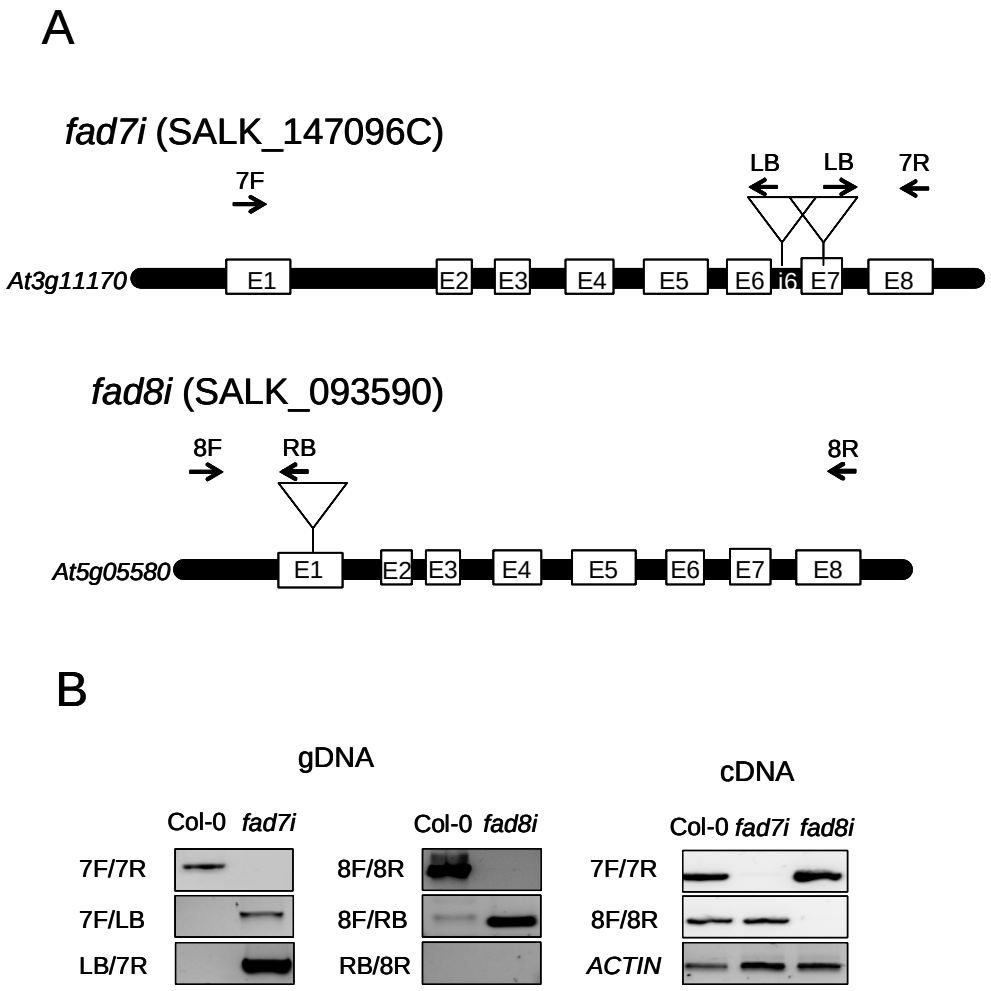

Figure 1. **Genotypic characterization of the Arabidopsis insertional mutants *fad8i* (SALK_093590) and *fad7i* (SALK_147096C).** (A) Schematic diagram showing the localization of the T-DNA insertions in the mutants. Exons are shown as white boxes. The triangles are used to mark the insertions. The arrows indicate the primers used for genotyping and expression analysis. (B) Characterization by PCR of the insertions. Left panels (gDNA) and right panels (cDNA) from Col-0, *fad7i* and *fad8i* plants. *ACTIN* was used as a housekeeping gene.

Fig. 2. Román et al.

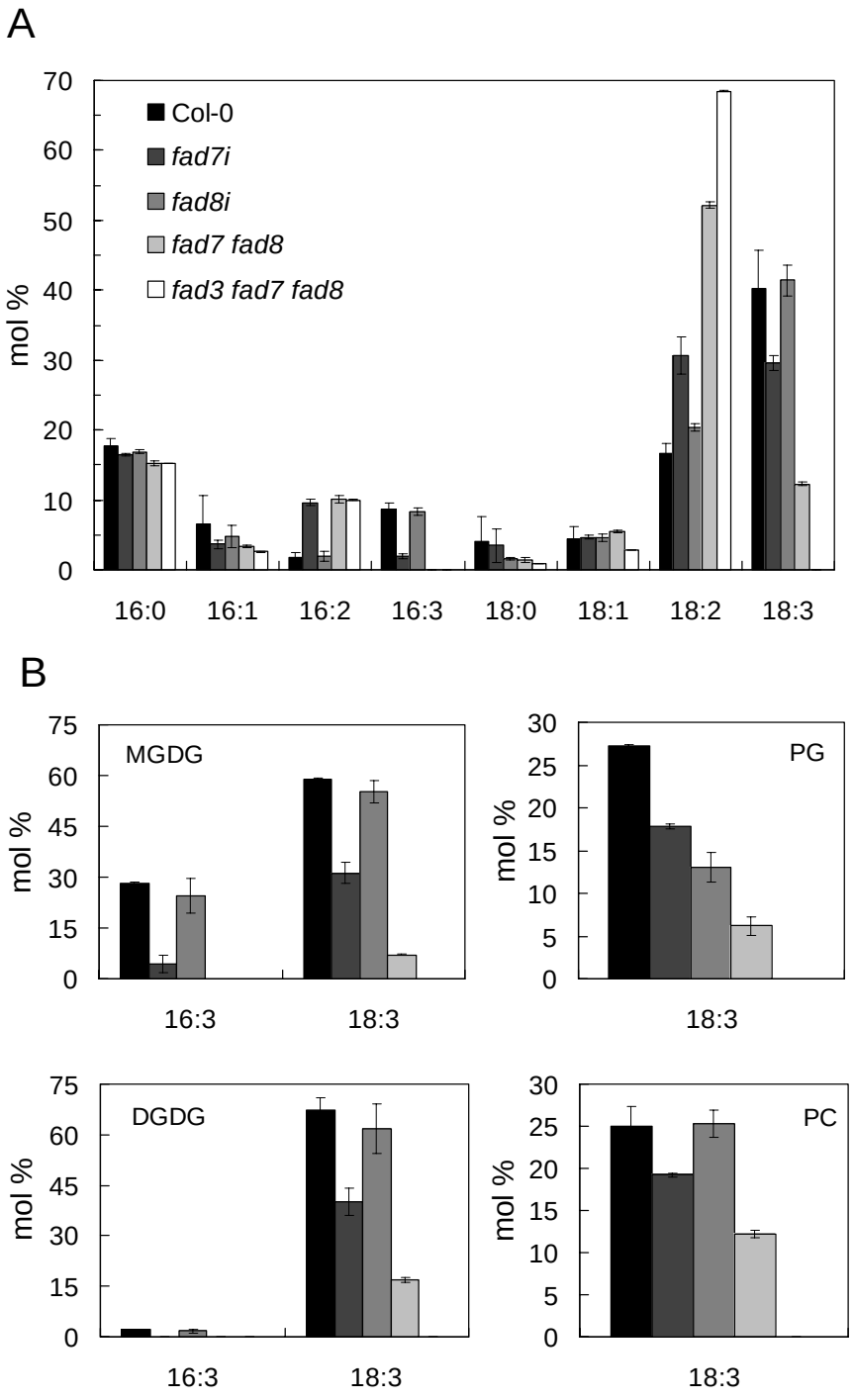

Figure 2. Fatty acid composition of total lipids and lipid classes from Arabidopsis Col-0 and mutant lines at 22 ºC. (A) Fatty acid composition of total lipids from Arabidopsis Col-0 and mutant lines (*fad7i*, *fad8i*, *fad7 fad8* and *fad3 fad7 fad8*) grown at 22 ºC. (B) Trienoic fatty acids content in MGDG, DGDG, PC and PG lipid classes. Data are mean of three biological experiments with two technical repeats for each experiment.

Fig. 3. Román et al.

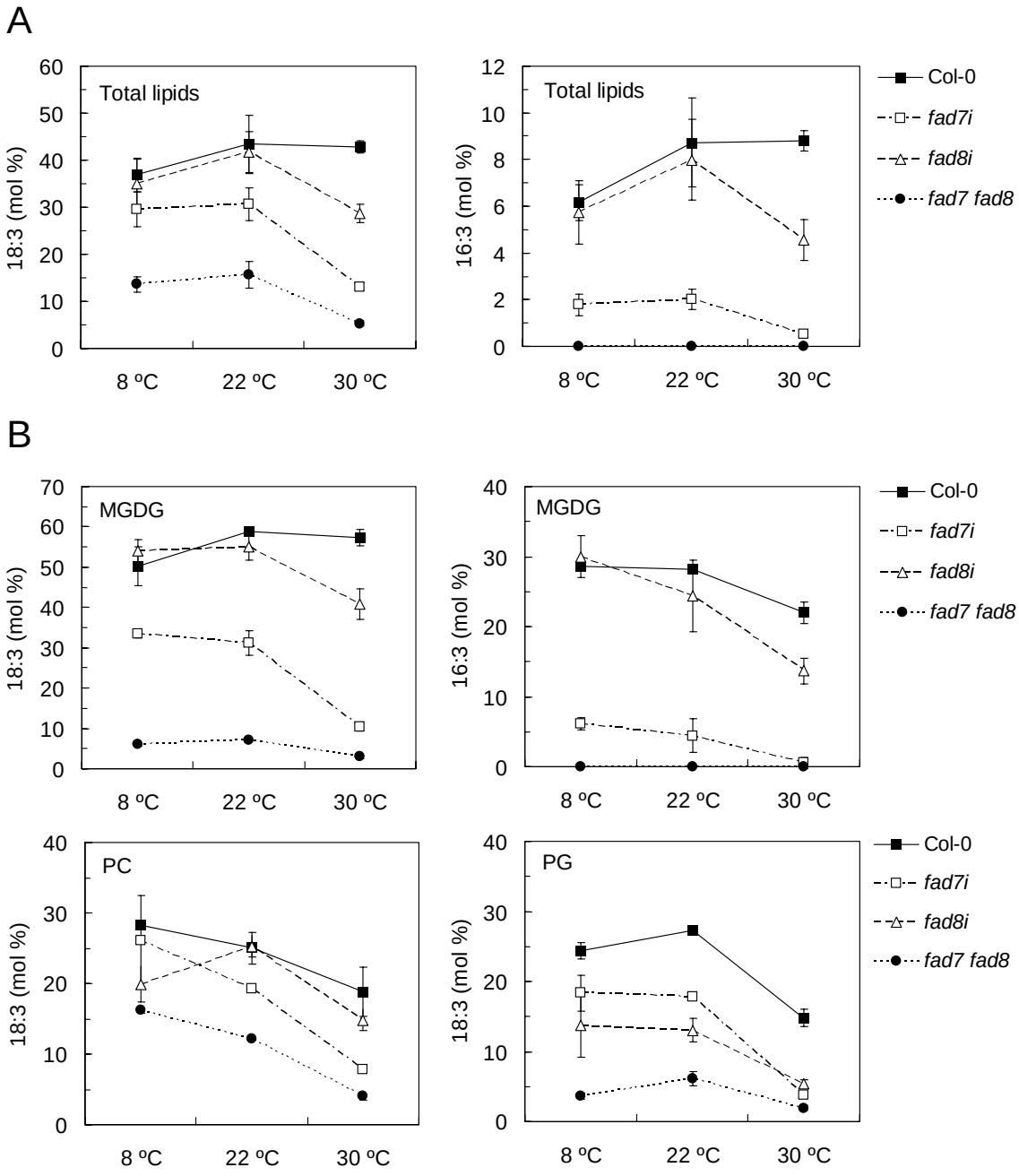

Figure 3. Trienoic fatty acid content of total lipids and lipid classes from Arabidopsis Col-0 and mutant lines grown at 8, 22 and 30 ºC. (A) Trienoic fatty acid composition of total lipids from Arabidopsis Col-0 and mutant lines (*fad7i*, *fad8i*, *fad7 fad8*) grown at 8, 22 and 30 ºC. (B) Trienoic fatty acid content in MGDG, PC and PG from Col-0 and mutant lines. Data are mean of three biological experiments with two technical repeats for each experiment.

Fig. 4. Román et al.

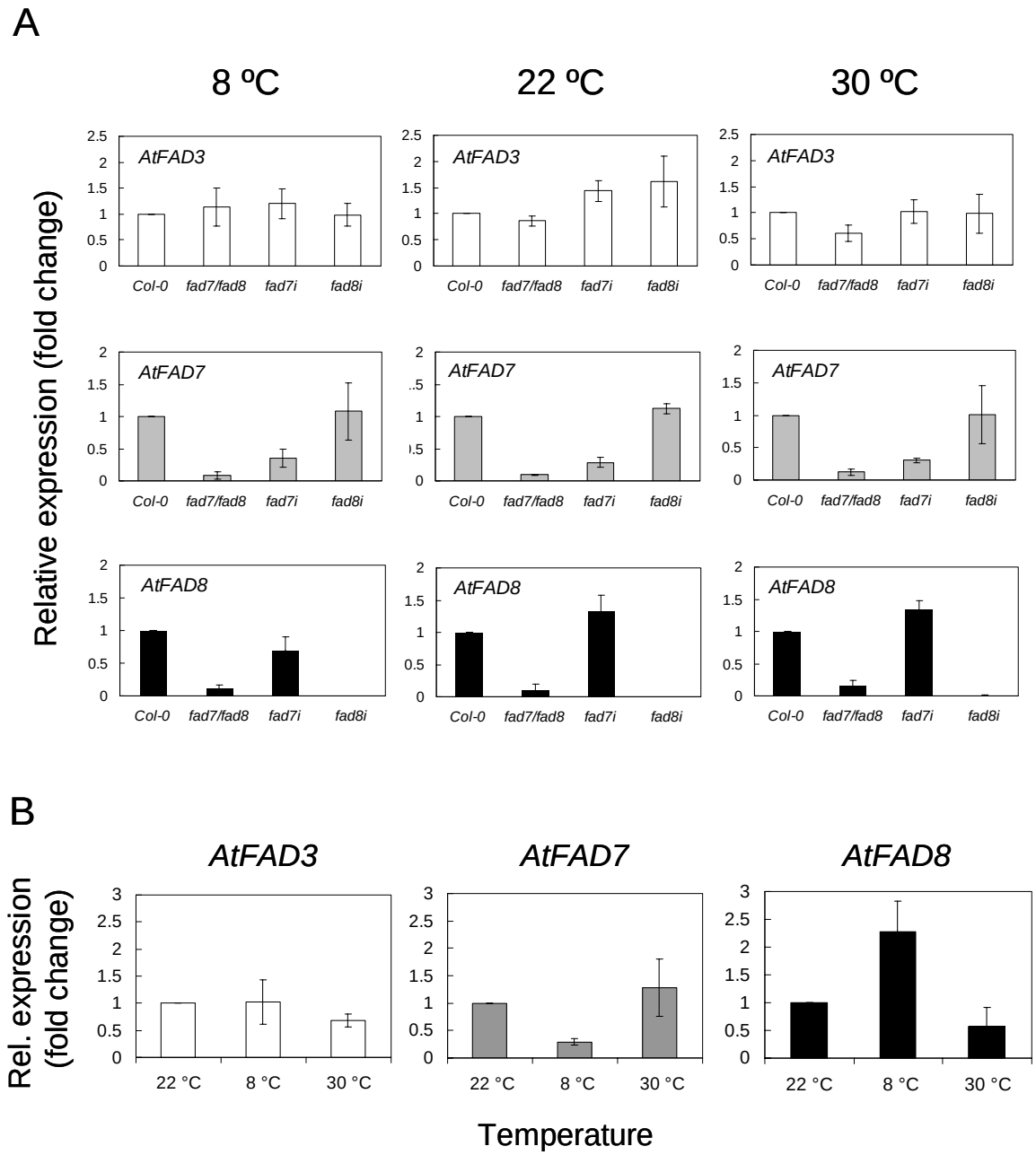

Figure 4. Expression of the *AtFAD8*, *AtFAD7* and *AtFAD3* genes from Col-0 and mutant lines at 22, 8 and 30 ºC. (A) q-PCR expression data of the *AtFAD8*, *AtFAD7* and *AtFAD3* genes from Col-0 and *fad7i*, *fad8i*, *fad7 fad8* and *fad3 fad7 fad8* mutants grown at 22, 8 and 30 ºC. Data were calibrated relative to the corresponding gene expression level in Col-0 (B) q-PCR expression data of *AtFAD8*, *AtFAD7* and *AtFAD3* genes from Col-0 plants grown at 22, 8 and 30 ºC. Data were calibrated relative to the corresponding gene expression level at 22 ºC. *EF1-α* was used as a housekeeping gene. Data are mean ± SD of 3 biological replicates with at least three technical repeats for each experiment.

Fig. 5. Román et al.

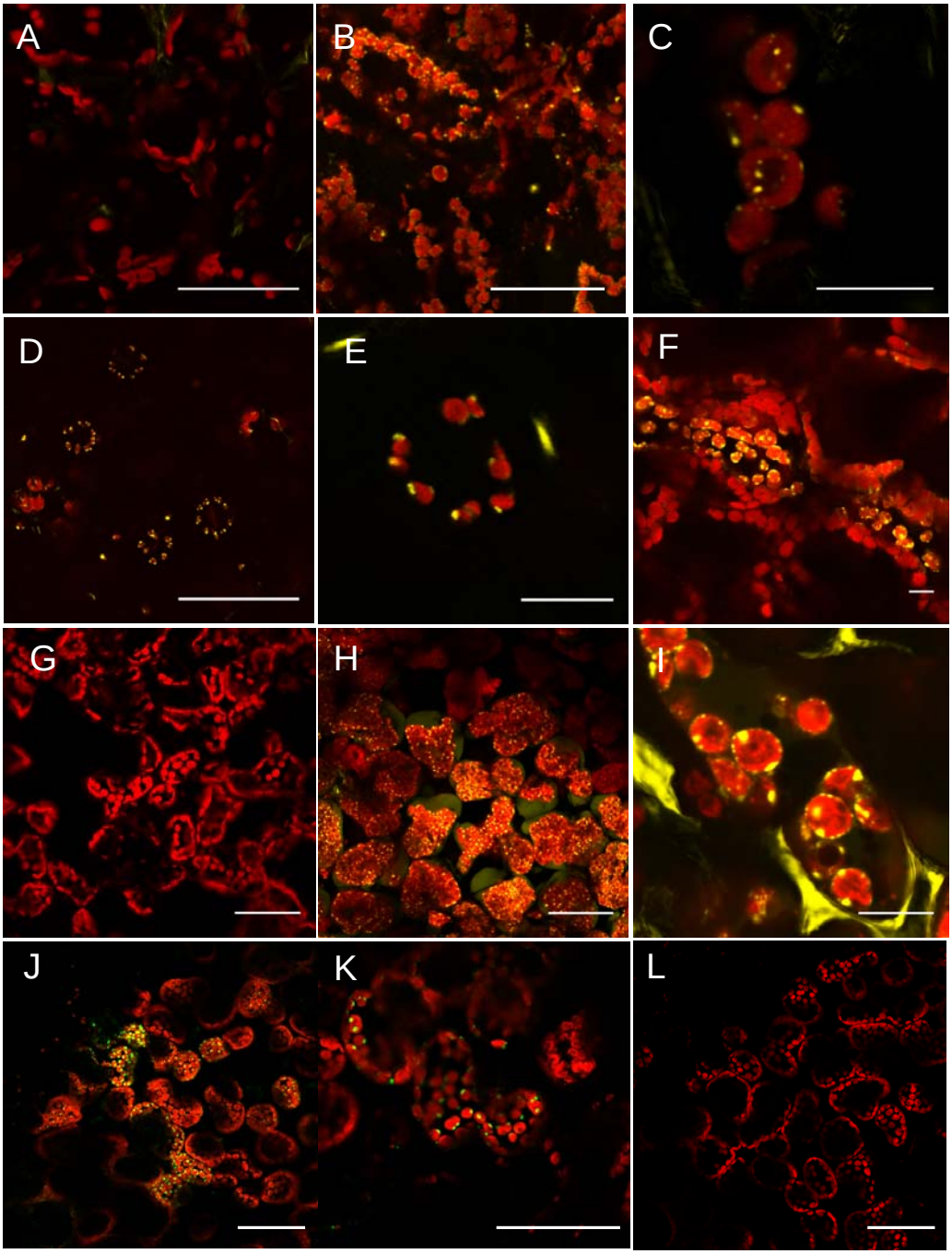

Figure 5. Expression of *At*FAD8-YFP fusion protein in stable transgenic Arabidopsis lines and transiently in *N. benthamiana* leaves. (A-F) Transgenic Arabidopsis lines: (A) leaves from plant transformed with the pEarley101 empty vector. (B-F) Leaves from plants transformed with FAD8-YFP fusion protein. (B), (C) and (F), mesophyll cells; (D) and (E), guard cells. (G-I), transient expression assay in *N. benthamiana* leaves: (G) plant transformed with the pEarley101 empty vector. (H) and (I) plants transformed with *At*FAD8-YFP fusion protein. (J-K) plants transformed with Tic40-GFP fusion protein as a control for positive envelope localization, (L) plants harbouring the empty pMDC83 vector. Scale bar is 50 µm in pictures A, B, D, F, G, H, J, and L, and 10 µm in pictures C, E, I, and K.

Fig. 6. Román et al.

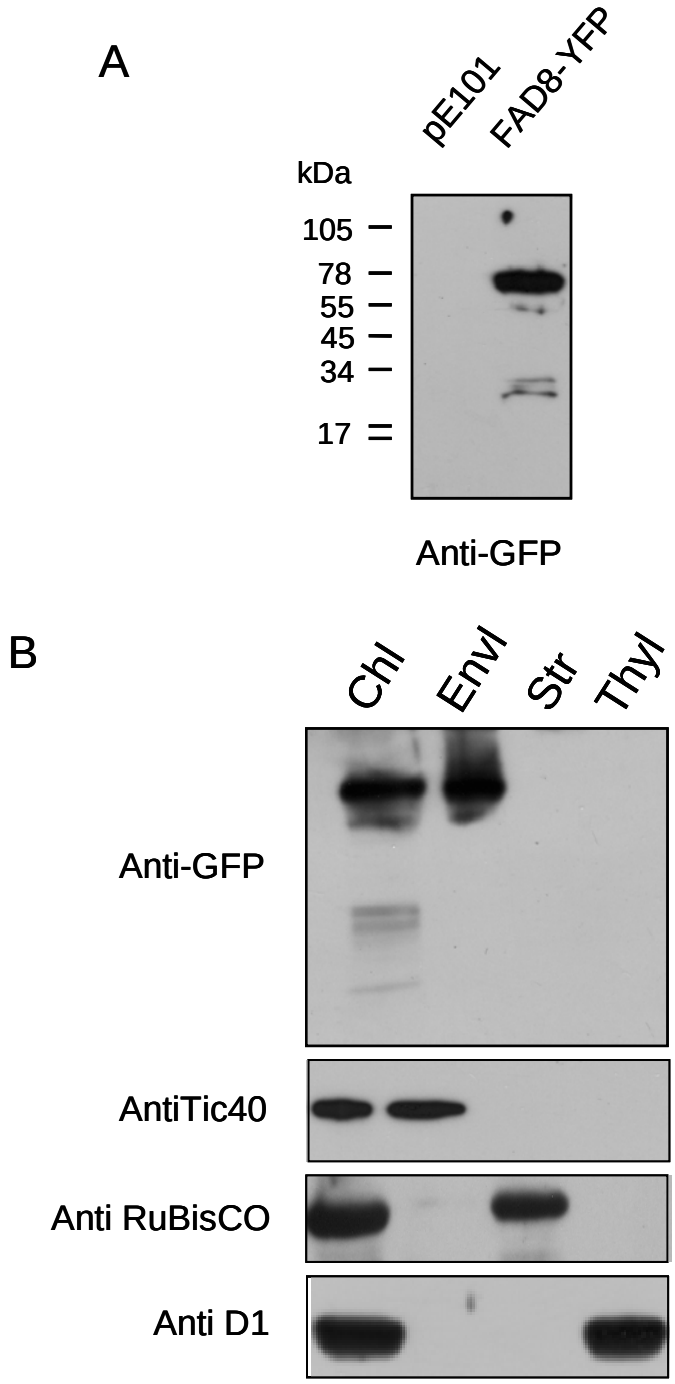

Figure 6. Expression and accumulation of the FAD8-YFP fusion protein. (A) Western blot using an anti-GFP antibody in chloroplasts isolated from plants transformed with the empty vector (pE101) and with the 35S:FAD8-YFP construct. Total protein of 10 μg was loaded per lane. (B) Biochemical fractionation of isolated chloroplasts from FAD8-YFP over-expressing lines. Chl, chloroplasts; Env, envelope; Str, stroma, Thyl, thylakoid fractions. Anti-Tic40, anti-RuBisCO and anti-D1 were used as protein markers of the envelope, stroma and thylakoid fractions from chloroplasts.

Fig. 7. Román et al.

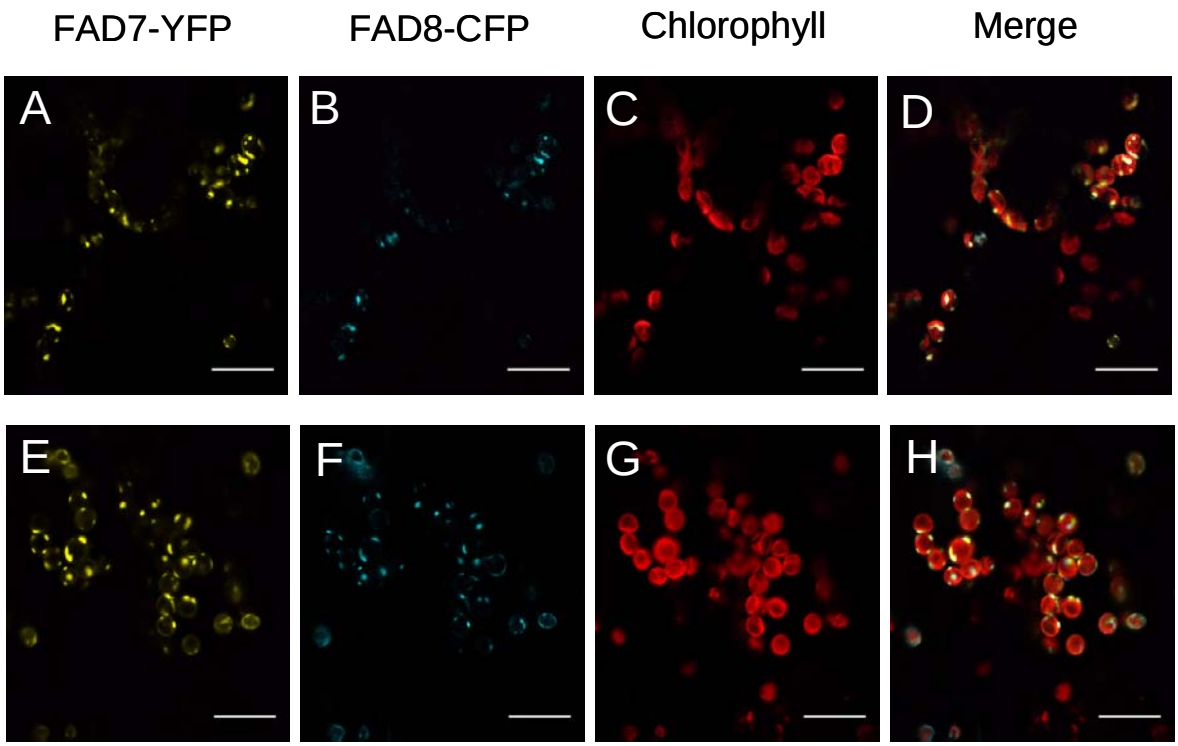

Figure 7. **Co-localization analysis of FAD8-CFP and FAD7-YFP fusion proteins by transient expression in *N. benthamiana* leaves.** (A and F) FAD7-YFP, (B and G) FAD8-CFP, (C and H) autofluorescence of the chlorophyll from plastids, (D and I) merged image from A,B , C and F,G,H, respectively. Scale bar is 10 μm in all pictures.

Fig. 8. Román et al.

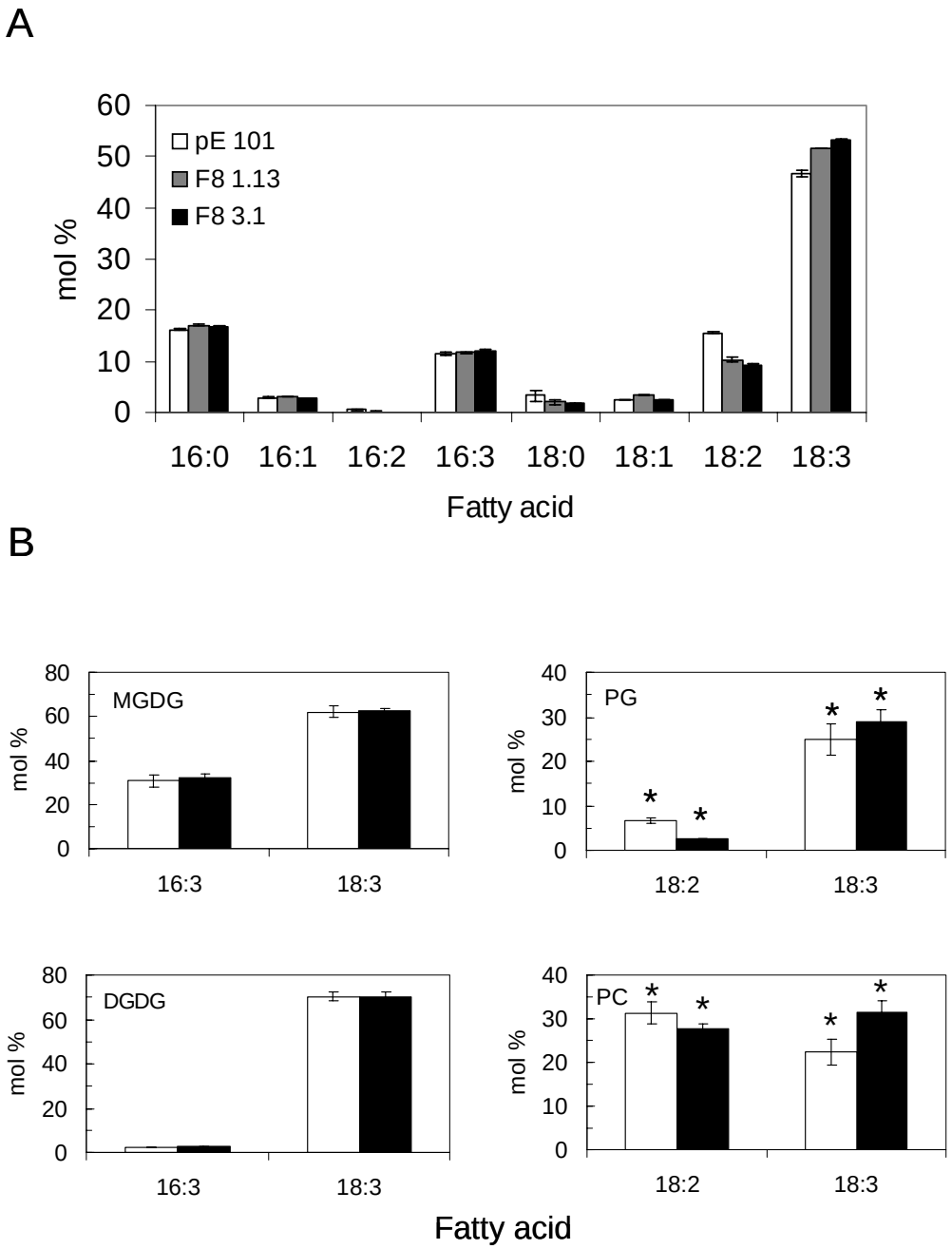

Figure 8. Fatty acid composition of total lipids and lipid classes from FAD8-YFP over-expressing lines grown at 22 ºC. (A) Total lipids in lines harbouring the empty pEarlyGate101 vector and F8 1.13 and 3.1 over-expressing the FAD8-YFP protein.(B) 16:3, 18:3 and 18:2 content in MGDG, DGDG, PC and PG. White bars represent plants carrying the empty pE101 vector and black bars F8 3.1 plants over-expressing the FAD8-YFP protein.